eLIFE elifesciences.org

RESEARCH ARTICLE

# Figures and figure supplements

Oxidative stress induces stem cell proliferation via TRPA1/RyR-mediated $Ca^{2+}$ signaling in the *Drosophila* midgut

**Chiwei Xu *et al***

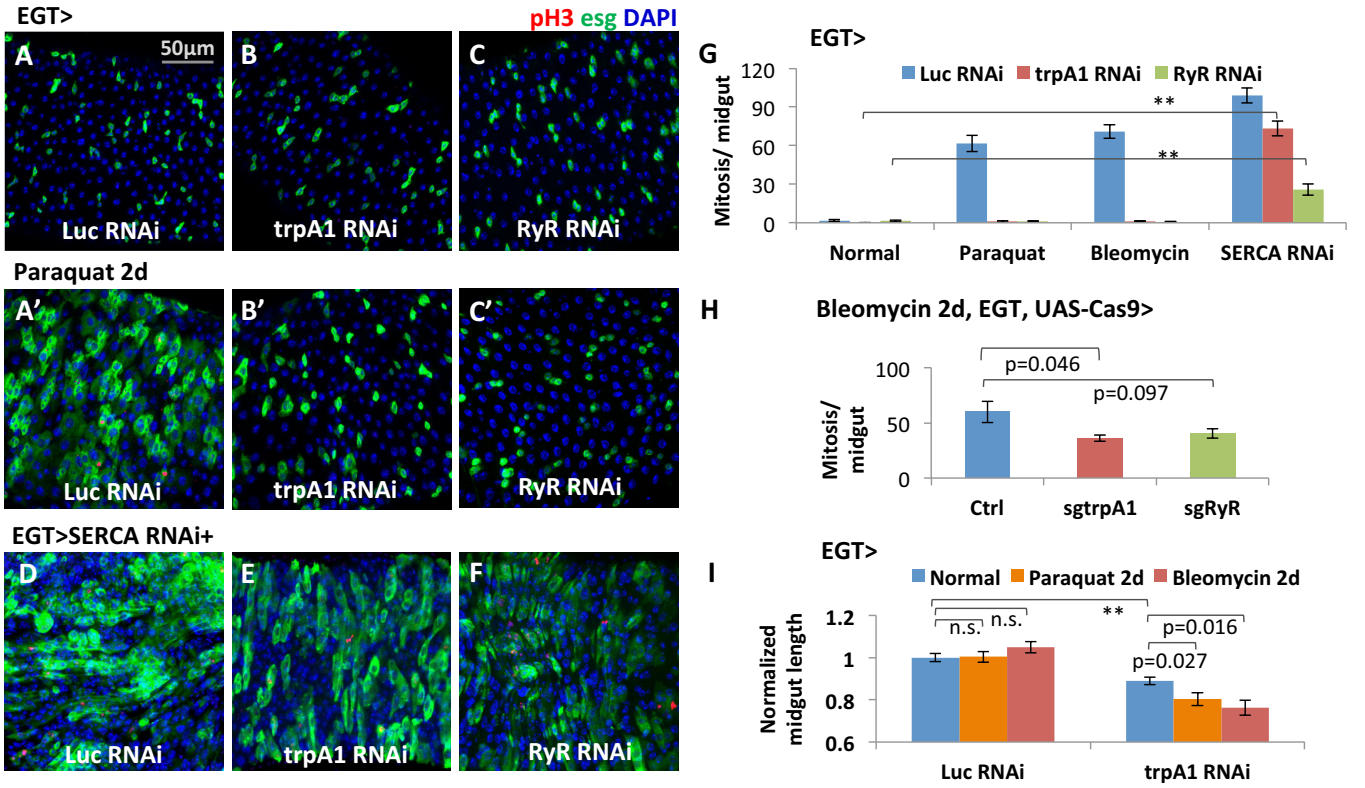


**Figure 1.** The calcium channels TRPA1 and RyR are required for damage-induced ISC proliferation. (**A–C**) Midguts overexpressing *Luc* RNAi, *trpA1* RNAi or *RyR* RNAi in ISCs using EGT (esgGal4 UAS-GFP tubGal80$^{ts}$) for 6d, were fed the oxidant agent paraquat for the last 2d (**A'–C'**) or co-expressed with *SERCA* RNAi (**D–F**). Midguts are stained for the mitosis marker phosphohistone H3 (pH3). *Luc* RNAi is used as control. $^{ts}$ stands for temperature sensitive tubGal80ts that allows for temporal control of genetic manipulation. GFP is used to report the expression pattern of esgGal4. (**G**) Quantification of mitosis (pH3+ cell number) of midguts expressing *Luc* RNAi, *trpA1* RNAi or *RyR* RNAi in ISCs under normal condition, 2 mM paraquat feeding, 25 μg/ml bleomycin feeding, or co-expression with *SERCA* RNAi. N > 5 midguts are quantified per genotype per treatment. Data are represented as mean ± SEM. Double asterisks indicate a p value of less than 0.01. (**H**) Mitosis quantification of midguts with constitutive expression of sgRNA targeting *trpA1* or *RyR*, and targeted Cas9 expression in ISCs for 7d (bleomycin feeding for the last 2d). Flies with the same genetic background but only empty insertional landing site are used as the control for sgRNA. Data are represented as mean ± SEM. Note that we generally observed that CRISPR/Cas9-mediated knockout in vivo is not working as efficiently as RNAi, probably because not all DNA damages by CRISPR/Cas9 result in frame-shift mutations. N > 6 midguts are analyzed per genotype. Data are represented as mean ± SEM. (**I**) Length quantification of midguts expressing *Luc* RNAi (control) or *trpA1* RNAi for 7d, with the last 2d feeding on normal food, paraquat, or bleomycin. The average midgut length of control flies feeding on normal food is used for normalization. N > 5 midguts are analyzed per genotype per treatment. Data are represented as mean ± SEM.
DOI: 10.7554/eLife.22441.002
The following source data is available for figure 1:

**Source data 1.** Complete results for ***Figure 1G–I***, ***Figure 1—figure supplement 1E***, ***Figure 1—figure supplement 3A–B***.
DOI: 10.7554/eLife.22441.003

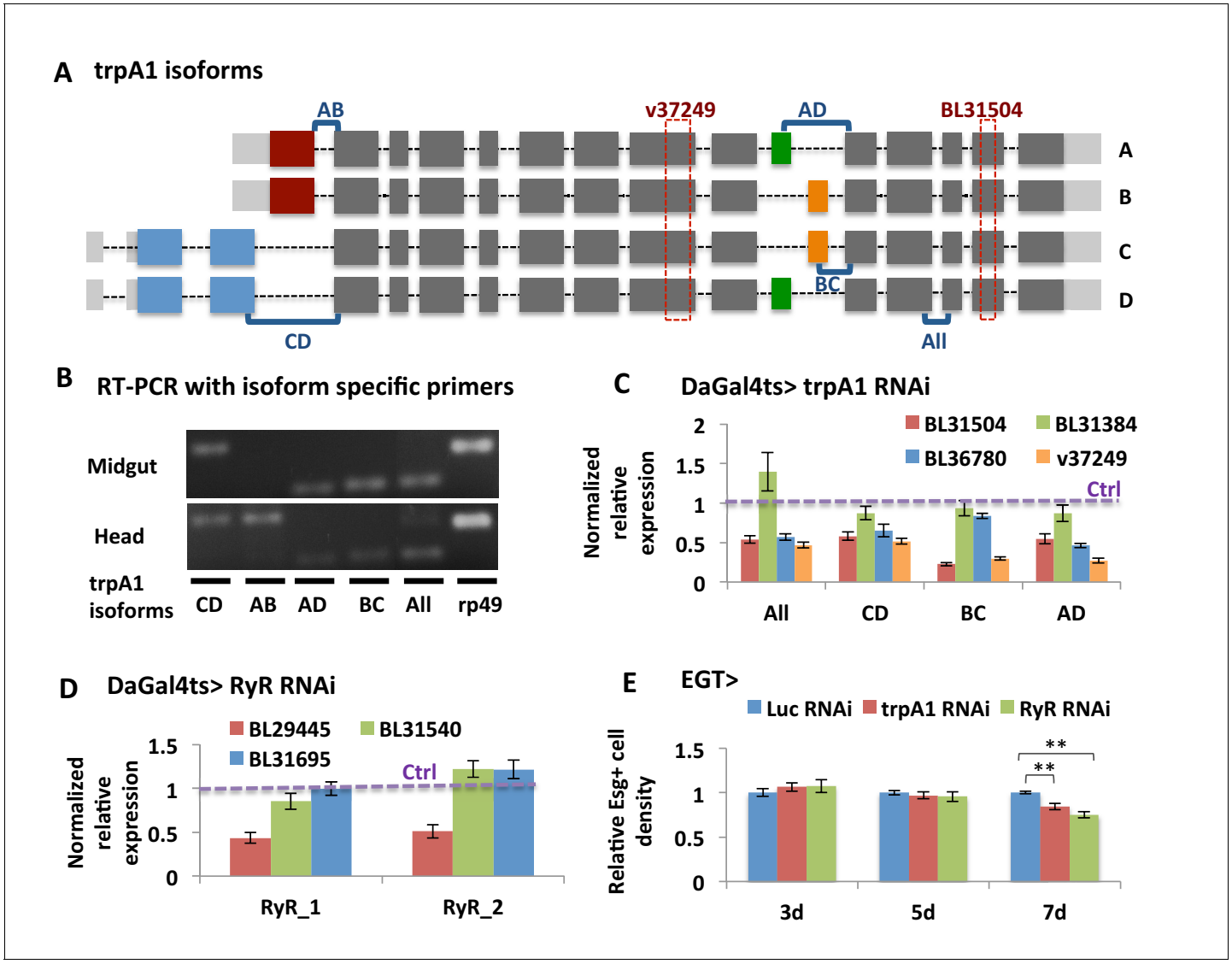


**Figure 1—figure supplement 1.** Validation of knockdown efficiency for *trpA1* RNAi and *RyR* RNAi lines. (**A**) Cartoon depicting the four characterized *trpA1* isoforms. The target regions of *trpA1* RNAi lines used in this study are shown in dashed rectangles. The regions amplified with isoform-specific primers are shown in square brackets. (**B**) Primers spanning exons for specific splicing events are used in RT-PCR to distinguish *trpA1* isoform expression in fly midguts and heads. (**C**) RT-qPCR analysis of mRNAs from midguts expressing different lines of *trpA1* RNAi ubiquitously with inducible DaGal4ts for 5d, with primers designed for different types of *trpA1* isoforms. *GAPDH* and *rp49* are reference genes for normalization. To determine RNAi knockdown efficiency, the ratio of normalized *trpA1* expression to corresponding control groups expressing either *Luc* RNAi (for BL lines) or carrying an empty insertional landing site (v60100 for v37249) is calculated. The data are presented as mean ± SEM for three technical replicates. We repeated the experiments (two biological replicates) and observed consistent results. (**D**) RT-qPCR measurement of midguts ubiquitously expressing *Luc* RNAi or *RyR* RNAi for 5d, with two different sets of primers designed for all *RyR* isoforms. *GAPDH* and *rp49* are used for normalization. The data are presented as mean ± SEM for three technical replicates. We repeated the experiments (two biological replicates) and observed consistent results. (**E**) Quantification of relative esg+ cell density in the posterior midgut region. esg+ cell number is divided by the imaged area size for density calculation. N > 5 midguts per genotype per time point are analyzed. Data are represented as mean ± SEM.

DOI: 10.7554/eLife.22441.004

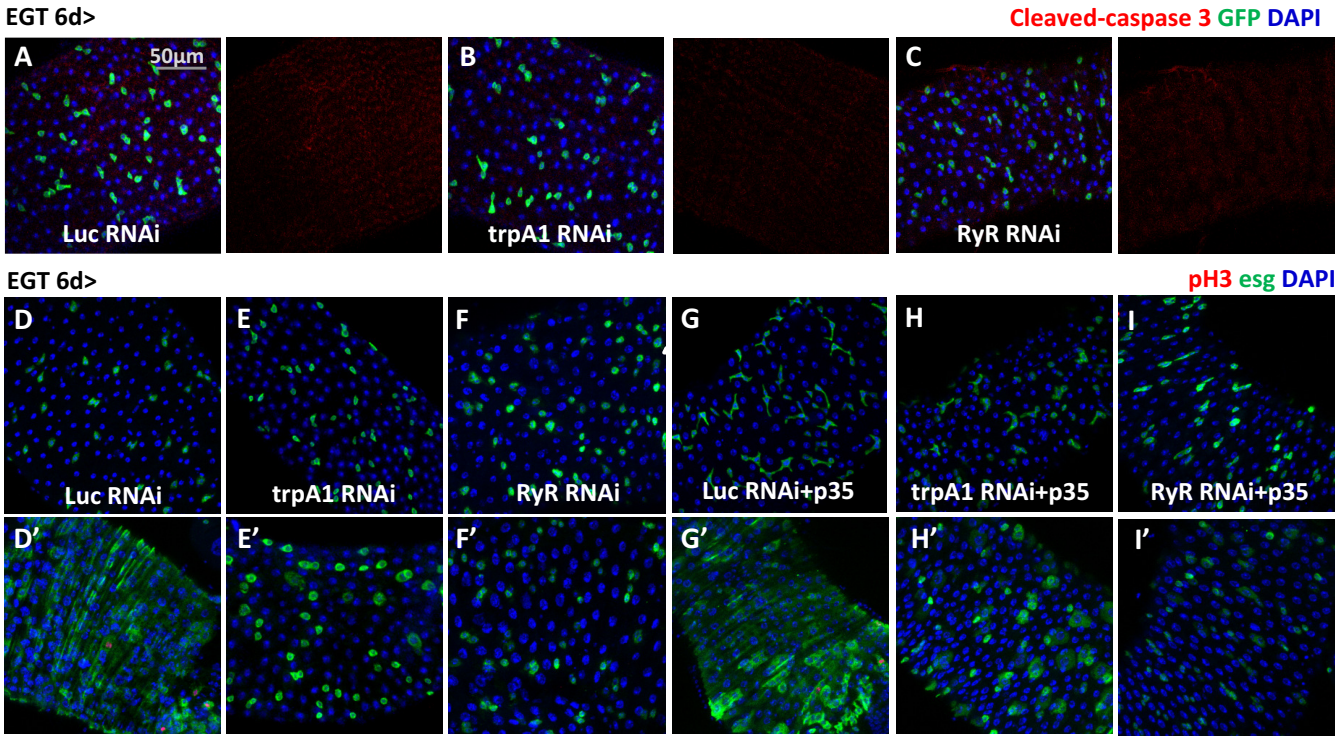


**Figure 1—figure supplement 2.** *trpA1* RNAi and *RyR* RNAi do not cause ISC apoptosis. (**A–C**) Immunostaining of midguts expressing *Luc* RNAi, *trpA1* RNAi or *RyR* RNAi in ISCs for apoptosis marker cleaved-caspase 3. The channels of cleaved-caspase 3 signal are shown to the right of the merged images. No signal can be detected except some background staining in the trachea and muscle. (**D–F**) Midguts expressing *Luc* RNAi, *trpA1* RNAi or *RyR* RNAi in ISCs with the last 2d feeding 2 mM paraquat (**D'–F'**), are stained for mitosis marker pH3. (**G–I**) Midguts expressing anti-apoptosis protein p35, together with *Luc* RNAi, *trpA1* RNAi or *RyR* RNAi in ISCs with the last 2d feeding 2 mM paraquat (**G'–I'**), are stained for mitosis marker pH3.
DOI: 10.7554/eLife.22441.005

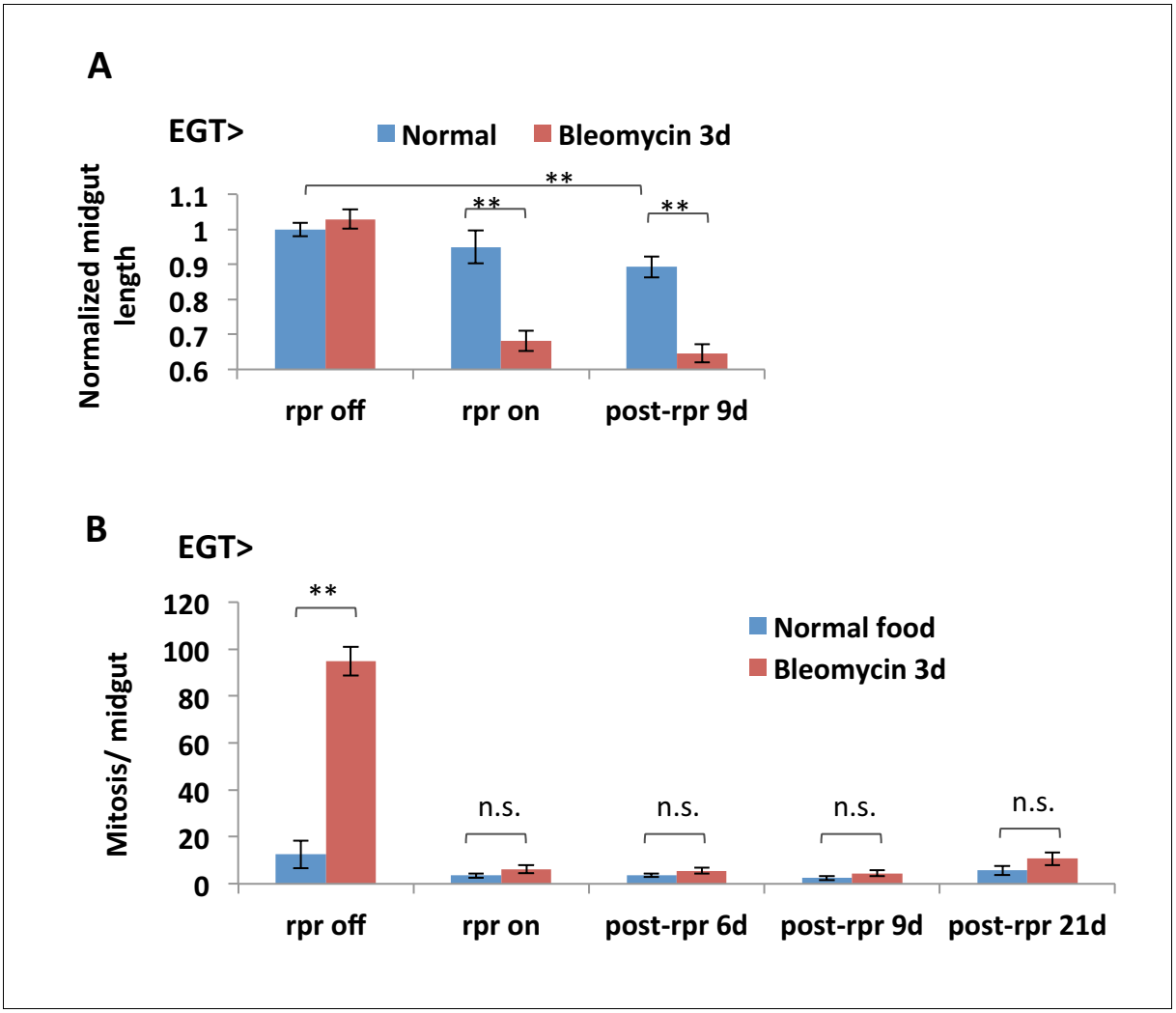


**Figure 1—figure supplement 3.** ISC depletion results in midgut shortening. (**A**) Length quantification of midguts with inducible expression of rpr in ISCs. In the 'rpr off' group, the flies are kept at 18˚C to prevent Gal4 activity and rpr expression; in the 'rpr on' group, rpr expression is induced at 29˚C for 4d and turned off at 18˚C for 3d feeding normal food or bleomycin; in the 'post-rpr' group, after 4d expression of rpr, the flies are placed back at 18˚C for specified days before bleomycin treatment. N > 6 midguts are analyzed per genotype per treatment. Data are represented as mean ± SEM. (**B**) Mitosis quantification of midguts with inducible expression of rpr in ISCs. Mitosis activity in the midgut cannot recover after depletion of the esg+ cell population by 4d rpr expression, N > 7 midguts are analyzed per genotype per treatment. Data are represented as mean ± SEM.
DOI: 10.7554/eLife.22441.006

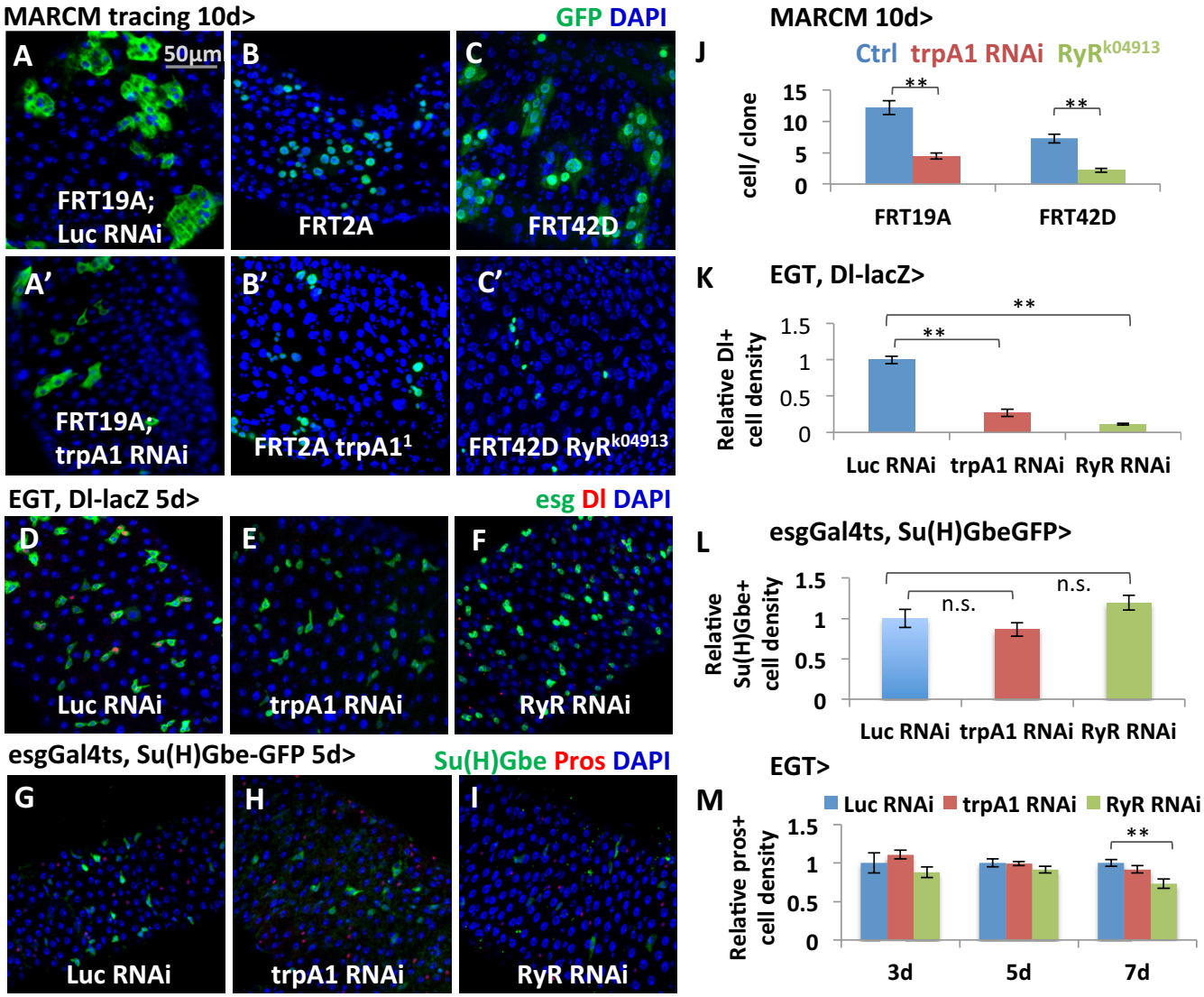


**Figure 2.** TRPA1 and RyR are required for ISC self-renewal but not differentiation. (**A–C, A'–C'**) MARCM clones deficient for TRPA1 or RyR are analyzed along with their corresponding control genotypes (A for A', B for B', C for C') 10d after clone induction. Cell numbers per clone for MARCM clones expressing *trpA1* RNAi, or lacking both wild-type *RyR* alleles, are quantified in (**J**). Randomly picked N = 35 clones from the posterior regions of five guts per genotype are analyzed. Data are represented as mean ± SEM. (**D–F**) ISC marker Dl-lacZ stainings of midguts expressing *Luc* RNAi, *trpA1* RNAi or *RyR* RNAi for 5d in ISCs. The relative Dl+ cell density in the posterior midgut region is quantified in (**K**). Dl+ cell number is divided by the imaged area size for density calculation. N > 5 midguts per genotype are analyzed. Data are represented as mean ± SEM. (**G–I**) Immunostaining of midguts expressing *Luc* RNAi, *trpA1* RNAi or *RyR* RNAi for 5d in ISCs for Notch activity reporter Su(H)GbeGFP and EE marker Prospero (pros). The relative Su(H)Gbe+ cell density in the posterior midgut region is quantified in (**L**). Su(H)Gbe+ cell number is divided by the imaged area size for density calculation. N > 4 midguts per genotype are analyzed. Data are represented as mean ± SEM. (**M**) Quantificatioin of EE density in the posterior midgut region for midguts expressing *Luc* RNAi, *trpA1* RNAi or *RyR* RNAi in ISCs for 3d, 5d, and 7d. For each time point, EE density is normalized to the average value of midguts expressing *Luc* RNAi. N > 4 midguts per genotype are analyzed. Data are represented as mean ± SEM.

DOI: 10.7554/eLife.22441.007

The following source data is available for figure 2:

**Source data 1.** Complete results for ***Figure 2J–M***.

DOI: 10.7554/eLife.22441.008

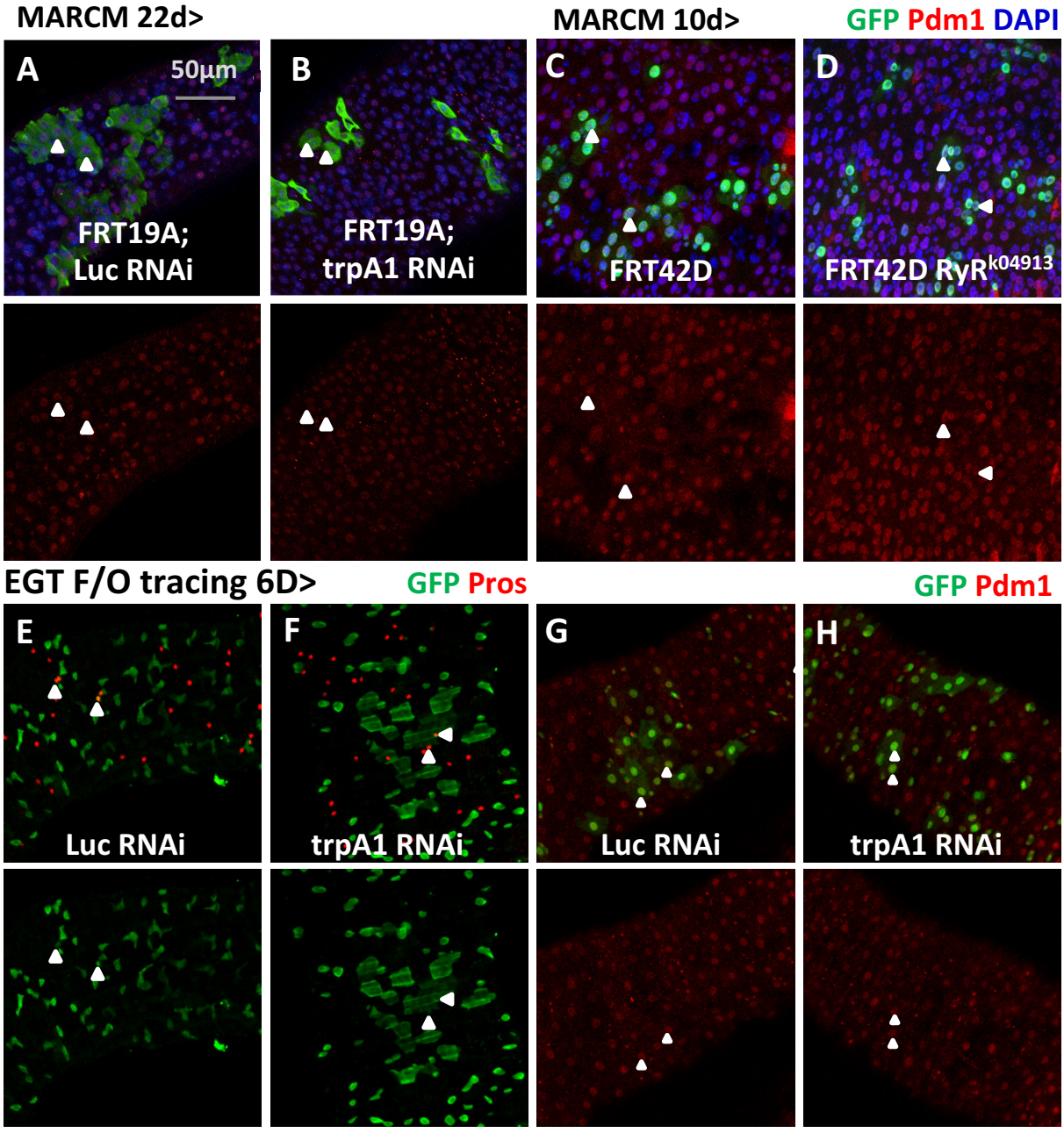


**Figure 2—figure supplement 1.** Lineage-tracing experiments provide evidence that TRPA1 or RyR-deficient ISCs can differentiate. (**A–B**) MARCM clones expressing *Luc* RNAi or *trpA1* RNAi for 22d are examined for their survival and stained with anti-Pdm1 antibody to examine EC differentiation. Arrowheads highlight examples of ECs generated from ISCs expressing *Luc* RNAi or *trpA1* RNAi. (**C–D**) MARCM clones that are homozygous RyR mutant are stained with anti-Pdm1 antibody. Arrowheads highlight examples of ECs in the MARCM clones that are Pdm1+. (**E–F**) Immunostaining of midguts expressing *Luc* RNAi or *trpA1* RNAi in the ISC lineage (labeled by GFP) for EE marker, Pros. Arrowheads highlight examples of EEs generated by ISCs during the 6d period of tracing. (**G–H**) Immunostaining of midguts expressing *Luc* RNAi or *trpA1* RNAi in the ISC lineage (labeled by GFP) for EC marker, Pdm1. Arrowheads highlight examples of ECs generated by ISCs during the 6d period of tracing.

DOI: 10.7554/eLife.22441.009

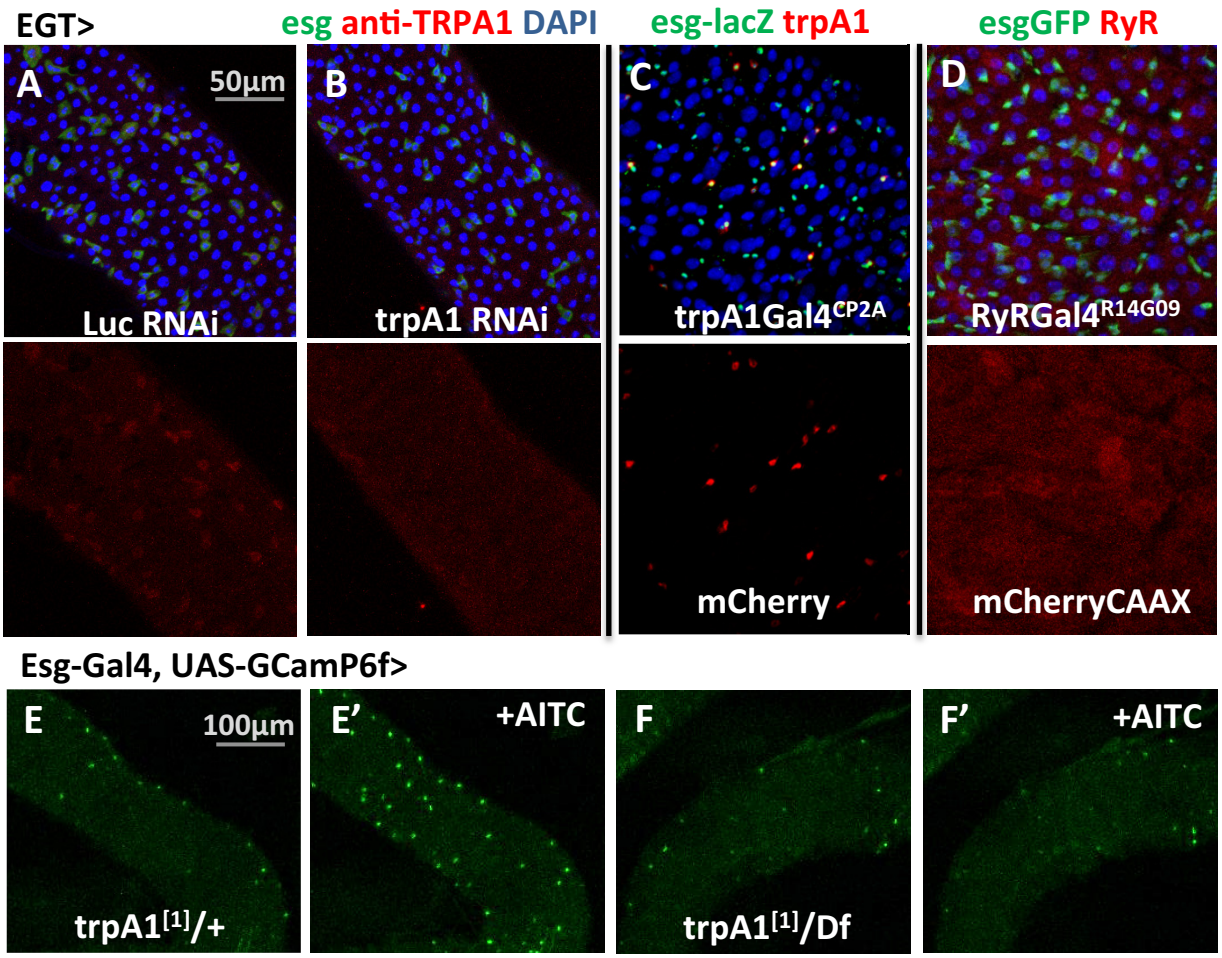


**Figure 3.** *trpA1* and *RyR* expression in the midgut. (**A–B**) Anti-TRPA1 immunostaining of midguts expressing *Luc* RNAi or *trpA1* RNAi in ISCs. The channel of anti-TRPA1 signal is shown below the merged image. Note that anti-TRPA1 staining has high background signal. While we could detect TRPA1 expression in the ISCs, we could not exclude the possibility that it is also expressed in other cell types. (**C**) *trpA1*Gal4$^{CP2A}$-driven expression of mCherry is co-stained with ISC marker esglacZ. (**D**) *RyR*Gal4$^{R14G09}$ (enhancer region of RyR locus) driven expression of membrane-localized CAAX-mCherry is co-stained with ISC marker esgGFP. (**E–F**) Imaging midguts missing one or both alleles of wild-type *trpA1* with GCaMP6f expression in ISCs. The same guts are imaged again after exposure to 0.015% AITC in the imaging buffer for 5 min (**E'–F'**). The images are acquired on a Keyence microscope.

DOI: 10.7554/eLife.22441.010

The following source data is available for figure 3:

**Source data 1.** Complete results for ***Figure 3—figure supplement 2B***.

DOI: 10.7554/eLife.22441.011

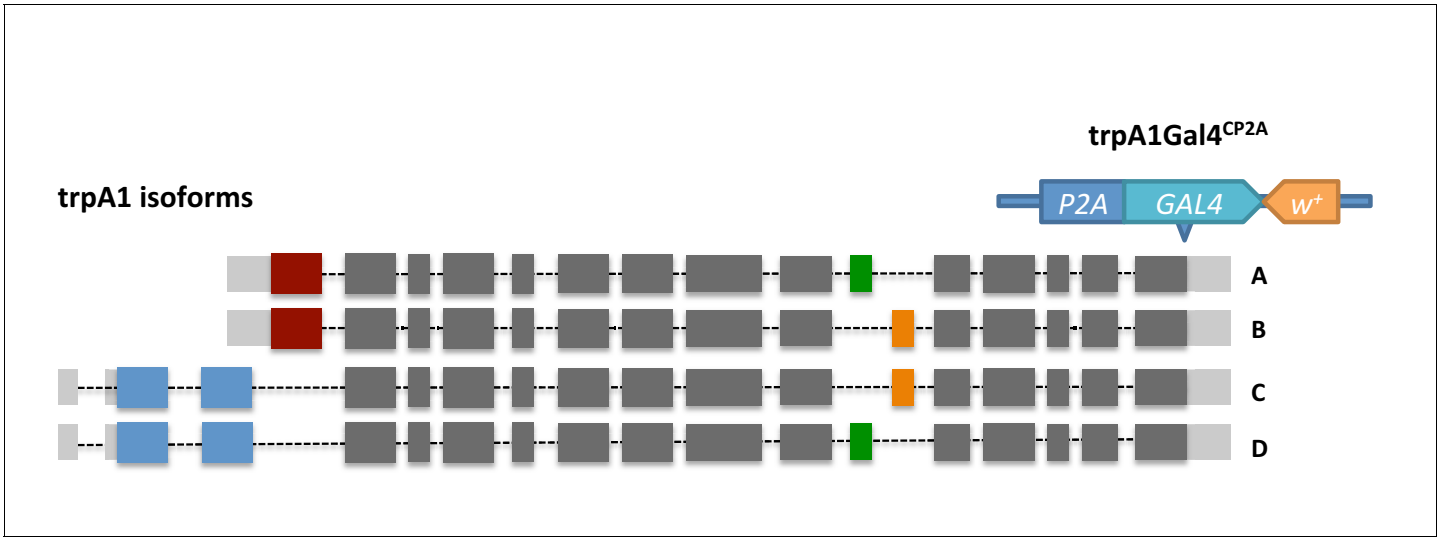


**Figure 3—figure supplement 1.** The knock-in design of *trpA1*Gal4$^{CP2A}$. By CRISPR/Cas9-induced homologous recombination, Gal4 is inserted into the shared C terminal of *trpA1* isoforms right before the stop codon. The knock-in could result in bi-cistronic transcripts expressing both TRPA1 and Gal4.
DOI: 10.7554/eLife.22441.012

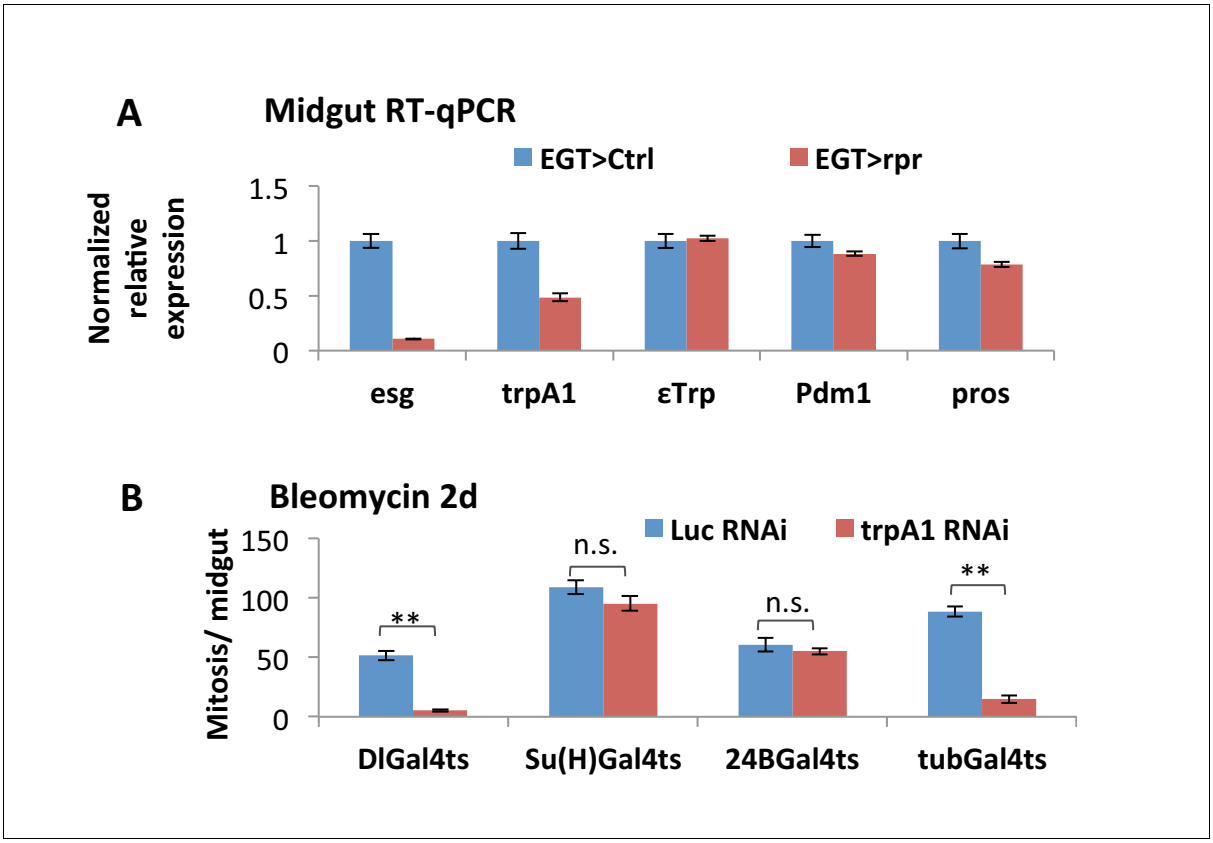


**Figure 3—figure supplement 2.** Additional evidence for *trpA1* expression and function in ISCs. (**A**) RT-qPCR measurement of midguts expressing the cell death gene *rpr* in ISCs for 4d for the expression of *esg*, *trpA1* (using primers for *CD* isoforms), EC marker *ε-Trpsin* (*εTrp*), *Pdm1*, or *pros*. *GAPDH* and *rp49* are used for normalization. The data are presented as mean ± SEM for three technical replicates. We repeated the experiments (two biological replicates) and observed consistent results. (**B**) Mitosis quantification of midguts expressing *Luc* RNAi or *trpA1* RNAi in self-renewing ISCs (DlGal4ts), differentiating ISCs or enteroblasts (Su(H)Gal4ts), muscles (24BGal4ts), or ubiquitously (tubGal4ts) for 9d, with last 2d feeding bleomycin. DlGal4ts and Su(H)Gal4ts are used to drive gene expression in ISCs and enteroblasts, respectively (***Zeng et al., 2010***). Data are represented as mean ± SEM.

DOI: 10.7554/eLife.22441.013

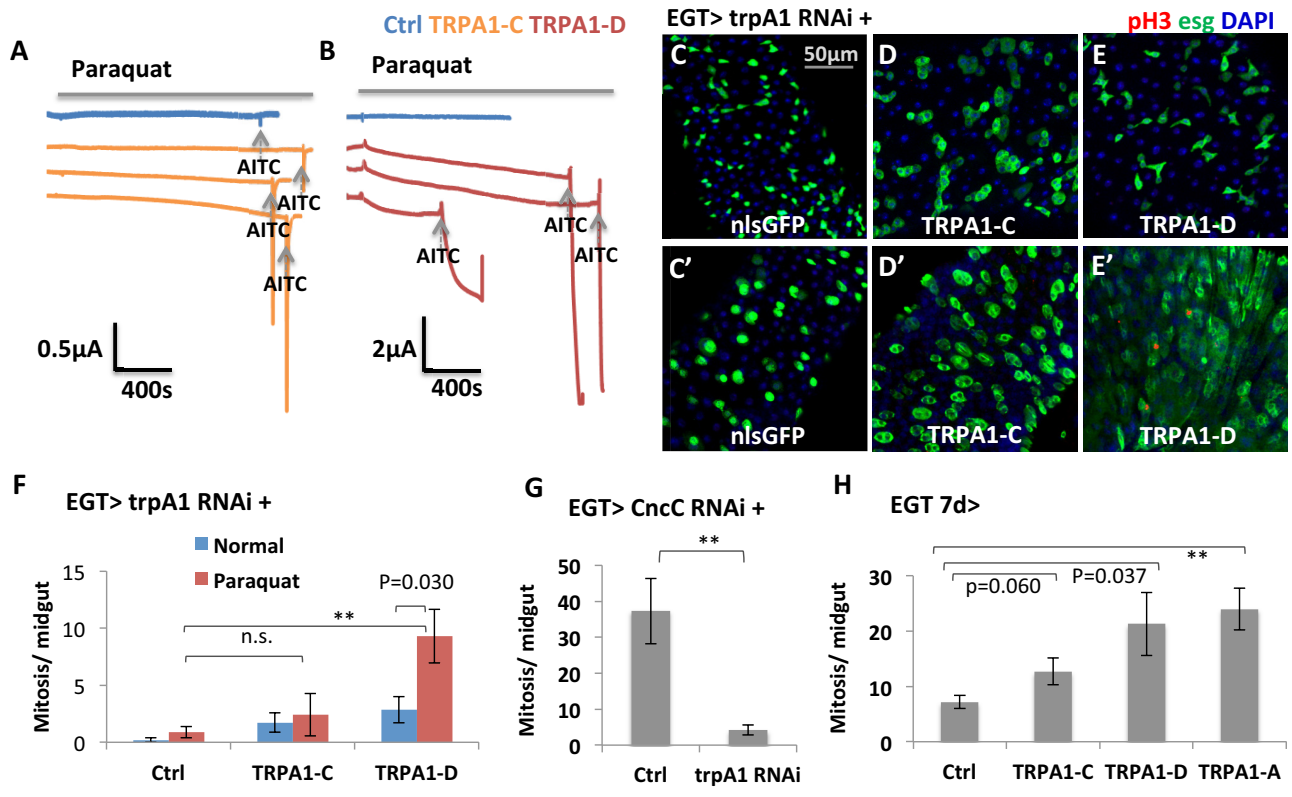


**Figure 4.** TRPA1 can respond to oxidant agent and its activation stimulates ISC activity. (**A–B**) Oocyte clamp measurement of TRPA1-C or TRPA1-D channel activities in response to paraquat. The same amounts of mRNAs for TRPA1-C or TRPA1-D were injected into Xenopus oocytes. 4 mM paraquat is present in the buffer during the period marked with the gray line on the top. Near the end of the experiment, the TRPA1 agonist AITC was added as a positive control (indicated with arrowhead). 2 mM and 10 mM paraquat were also tested and gave consistent results. (**C–E**) Midguts, expressing *trpA1* RNAi alone, or together with TRPA1-C or TRPA1-D in the ISCs for 7d, with the last 2d feeding paraquat (**C'–E'**), are stained for the mitosis marker pH3. Nucleus-localized GFP (nlsGFP) is used as the control for transgenic expression. We have also tested UAS-ultraGFP (***Yang and Tower, 2009***) that consists of multiple copies of UAS-2xEGFP as control and obtained the same results as UAS-nlsGFP with regard to stem cell activity (except that ultraGFP reporter is much brighter than nlsGFP). (**F**) Mitosis quantification of midguts expressing *trpA1* RNAi together with TRPA1-C or TRPA1-D under normal and paraquat-feeding conditions. N > 4 midguts per genotype per treatment are analyzed for quantification. UAS-ultraGFP is used as the control for transgenic expression. Data are represented as mean ± SEM. Note that TRPA1-C or TRPA1-D are still targeted by *trpA1* RNAi, which might limit their capacity to rescue *trpA1* RNAi. (**G**) Mitosis quantification of midguts expressing *CncC* RNAi alone, or together with *trpA1* RNAi in the ISCs for 7d. N > 7 midguts are analyzed for each genotype. Data are represented as mean ± SEM. (**J**) Mitosis quantification of midguts overexpressing TRPA1-C, TRPA1-D, or TRPA1-A in ISCs for 7d. N > 5 midguts per genotype are analyzed. Data are represented as mean ± SEM.

DOI: 10.7554/eLife.22441.014

The following source data is available for figure 4:

**Source data 1.** Complete results for ***Figure 4F–H***.

DOI: 10.7554/eLife.22441.015

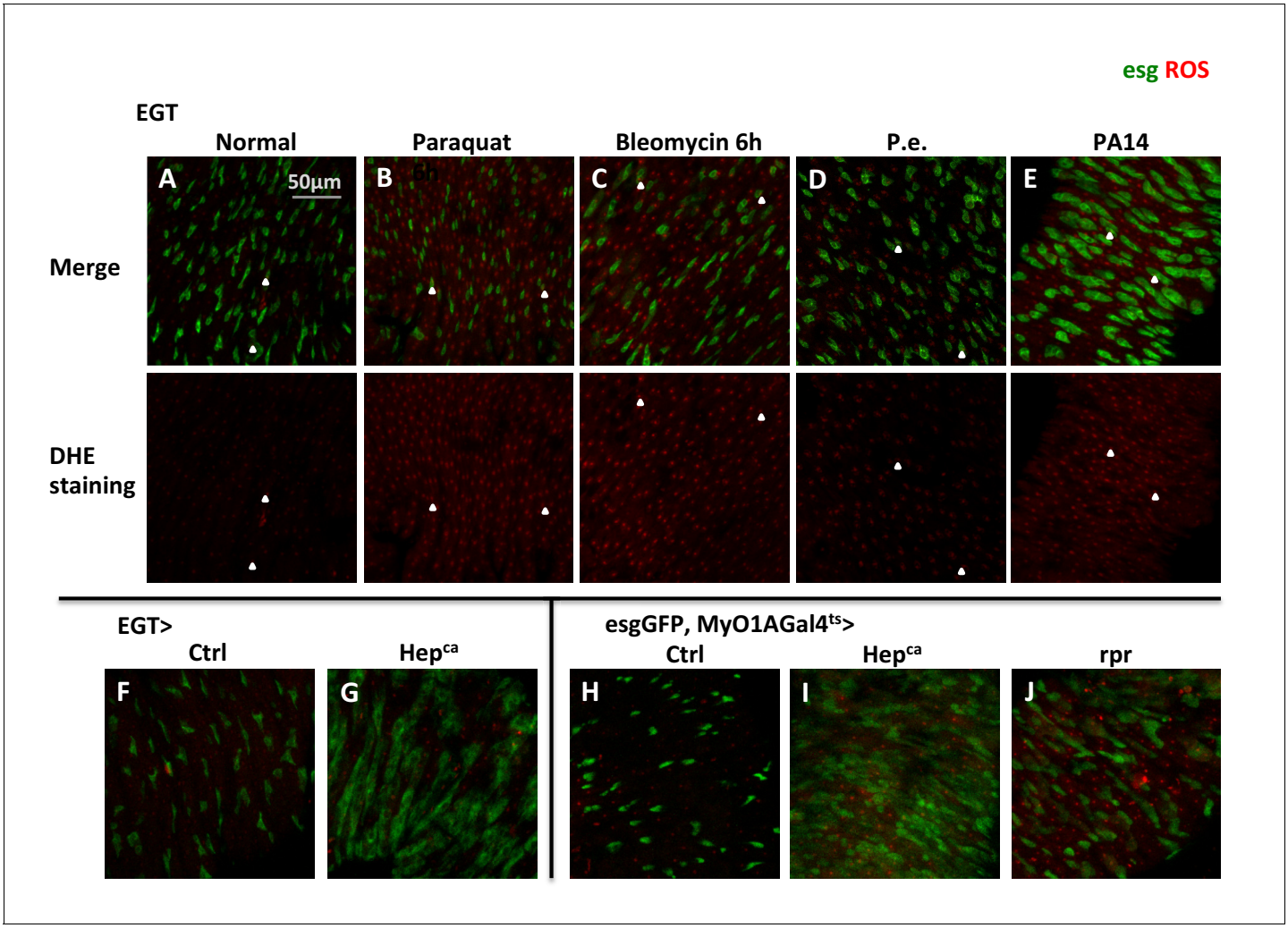


**Figure 4—figure supplement 1.** Elevated ROS is a common stress signal in various midgut damage conditions. (**A–E**) Dihydro-ethidium (DHE) stainings of live midguts expressing GFP in ISCs for 3d from flies fed with normal food, food containing 2 mM paraquat, 25 μg/ml bleomycin for 6 hr, pathogens *Pseudomonas entomophila* (P.e.), or *Pseudomonas aeruginosa* (PA14) for 18 hr. DHE signal channel is shown below the merged image. The control group for *Pseudomonas* infection, using Bacteria-free LB media, is not shown in the figure because the midgut DHE staining looks the same as flies fed with normal food. Arrowheads highlight examples of stem cells that have high ROS concentration. (**F–G**) DHE staining of midguts overexpressing active JNKK (*Drosophila* Hep$^{ca}$) for 1d in ISCs with EGT. (**H–J**) DHE staining of midguts overexpressing Hep$^{ca}$ or cell death gene *reaper* (*rpr*) for 2d in ECs with MyO1AGal4ts. esgGFP labels the ISCs.

DOI: 10.7554/eLife.22441.016

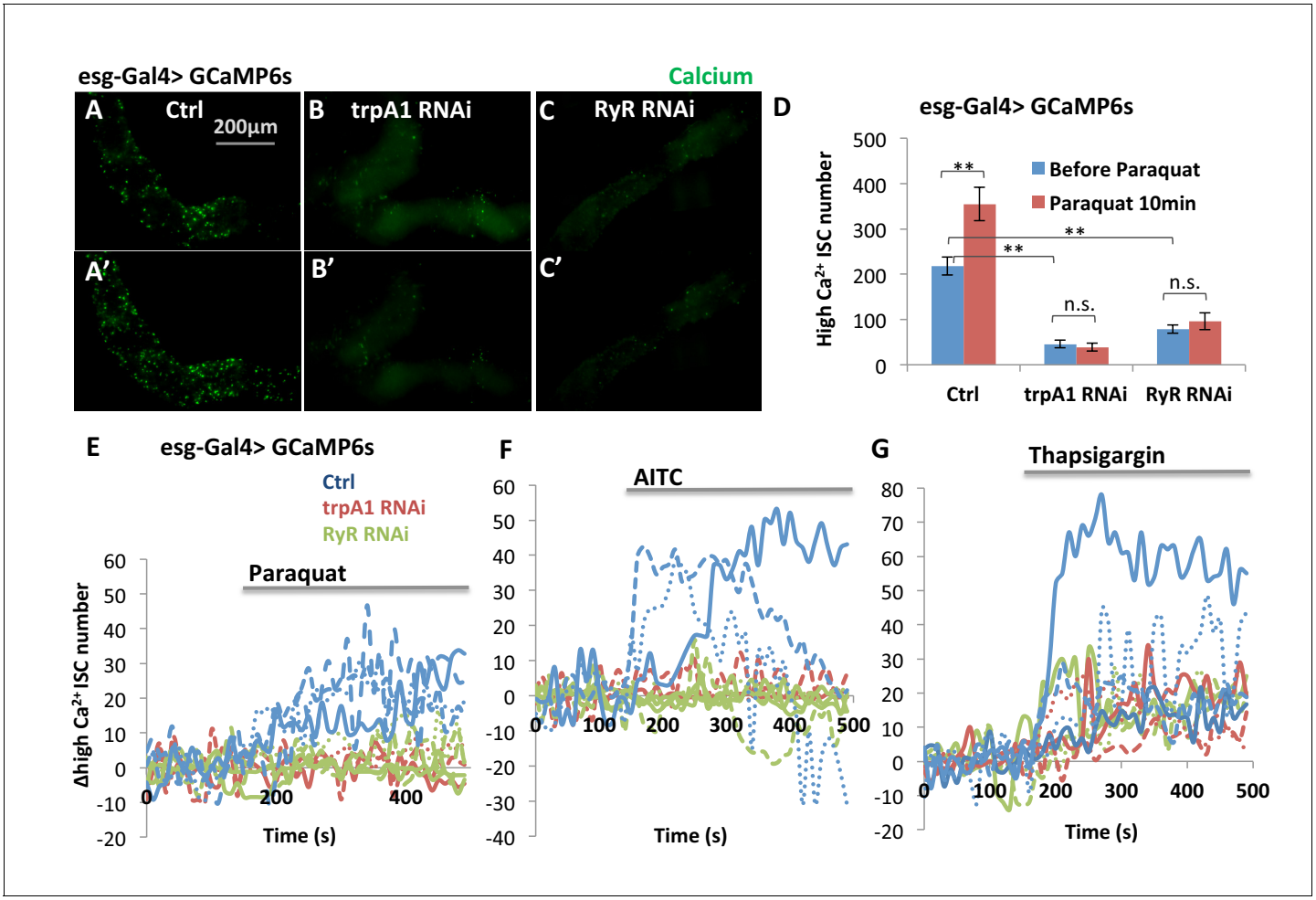


**Figure 5.** TRPA1 and RyR are required for ROS-mediated $Ca^{2+}$ increases in ISCs. (**A–C**) Imaging of midguts expressing the GCaMP6s reporter alone or together with *trpA1* RNAi or *RyR* RNAi in ISCs. The same guts are imaged again after exposure to 4 mM paraquat in the imaging buffer for 10 min (**A'–C'**). The images are acquired on a Keyence microscope. (**D**) Quantification of high $Ca^{2+}$ (GFP+) stem cells within the posterior midgut region. N > 5 midguts are analyzed for each genotype. Data are represented as mean ± SEM. (**E–G**) Numeric kinetics of high $Ca^{2+}$ stem cells in midguts expressing *trpA1* RNAi or *RyR* RNAi in ISCs. Wild-type midguts expressing GCaMP6s alone serve as control. Time-lapse confocal imaging is used for the analysis (see Supplementary Movies). The average number of high $Ca^{2+}$ stem cells before drug treatment is set as the basal level of 0 for individual imaging experiments. Final concentration of 4 mM paraquat (**E**), 0.03% AITC (**F**), 4 μM thapsigargin (**G**) are added at 150 s. At least three replicates of each genotypes/treatments are shown in the figure, with different colors labeling different genotypes.

DOI: 10.7554/eLife.22441.017

The following source data is available for figure 5:

**Source data 1.** Results for ***Figure 5D***, ***Figure 5—figure supplement 1D–E***, ***Figure 5—figure supplement 2F***.

DOI: 10.7554/eLife.22441.018

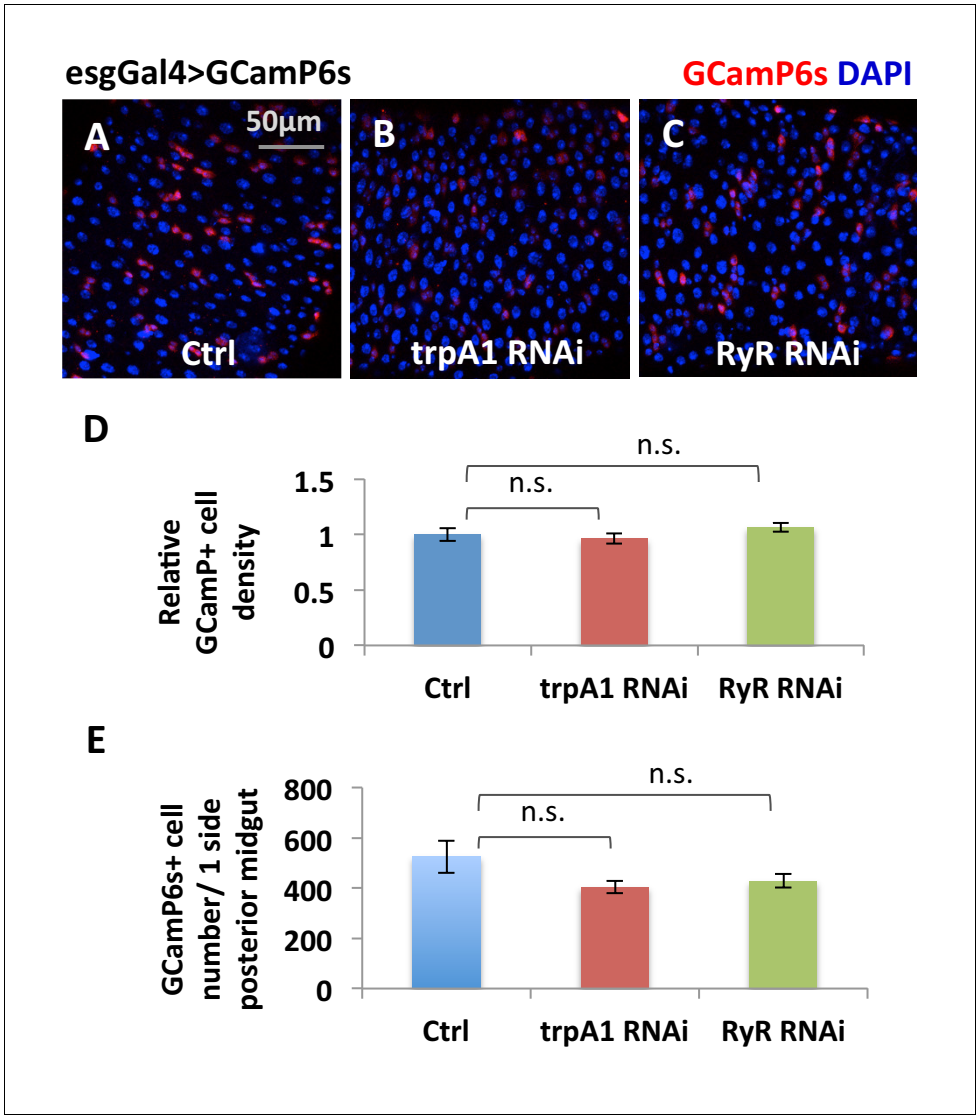


**Figure 5—figure supplement 1.** The total number of ISCs expressing esgGal4>GCamP6s reporter is not significantly reduced by *trpA1* RNAi or *RyR* RNAi. (**A–C**) Anti-GFP staining of midguts expressing GCamP6s alone, or together with *trpA1* RNAi or *RyR* RNAi in ISCs detects GCamP6s expression. The images are acquired on a confocal microscope. The relative density of GCamP6s+ (driven by esgGal4) cells, imaged on a Keyence microscope covering most of the posterior midgut region, is quantified in (**D**) while the total number of GCamP6s + cells in the posterior midgut region is quantified in (**E**). N > 8 midguts are analyzed for each genotype. Data are represented as mean ± SEM.

DOI: 10.7554/eLife.22441.019

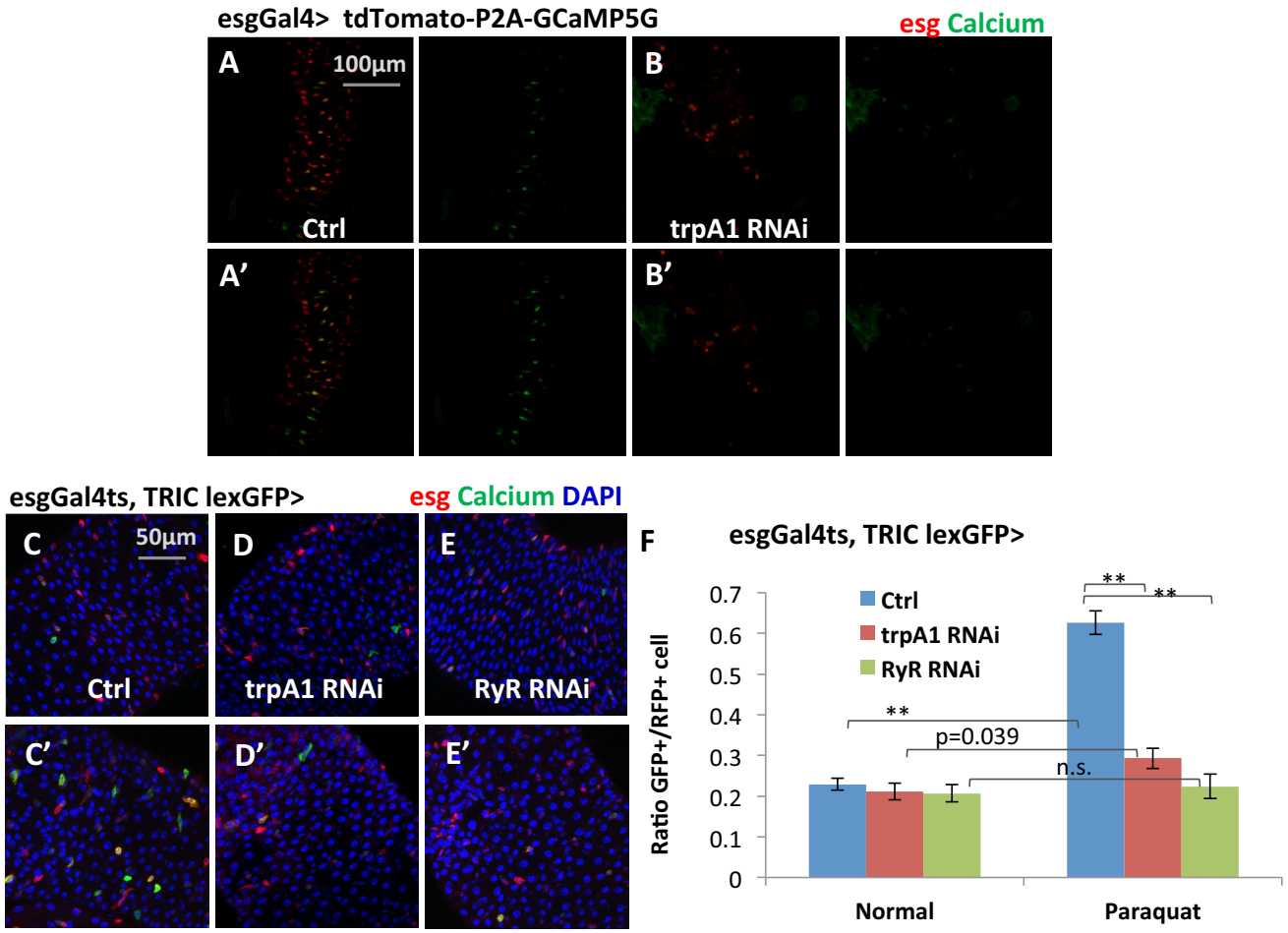


**Figure 5—figure supplement 2.** Additional reporters showing that TRPA1 and RyR are required for ROS-mediated $Ca^{2+}$ increases in ISCs. (**A–B**) Confocal calcium imaging of midguts that express bi-cistronic UAS-tdTomato-P2A-GCaMP5G reporter alone or together with *trpA1* RNAi in ISCs with exposure to 2 mM paraquat for 5 min (**A'–B'**). The bi-cistronic reporter consists of tdTomato that labels all cells expressing the reporter, and GCaMP5G whose GFP signal intensity reflects intracellular calcium concentration (***Daniels et al., 2014***). (**C–E**) Midguts expressing the TRIC lexGFP calcium reporter alone or together with *trpA1* RNAi or *RyR* RNAi in ISCs for 6d, with the last 1d feeding 2 mM paraquat (**C'–E'**) are stained to examine stem cell $Ca^{2+}$ concentration in vivo. The conventional *UAS*-RFP reporter is used to label all stem cells. (**F**) Quantification of high $Ca^{2+}$ stem cells (GFP+) ratio to all stem cells (RFP+) for midguts in experiments (**C–E**). N = 16, 10, six images are analyzed for the genotypes of control, *trpA1* RNAi, and *RyR* RNAi (half feeding normally, half feeding paraquat for 1d). Data are represented as mean ± SEM.

DOI: 10.7554/eLife.22441.020

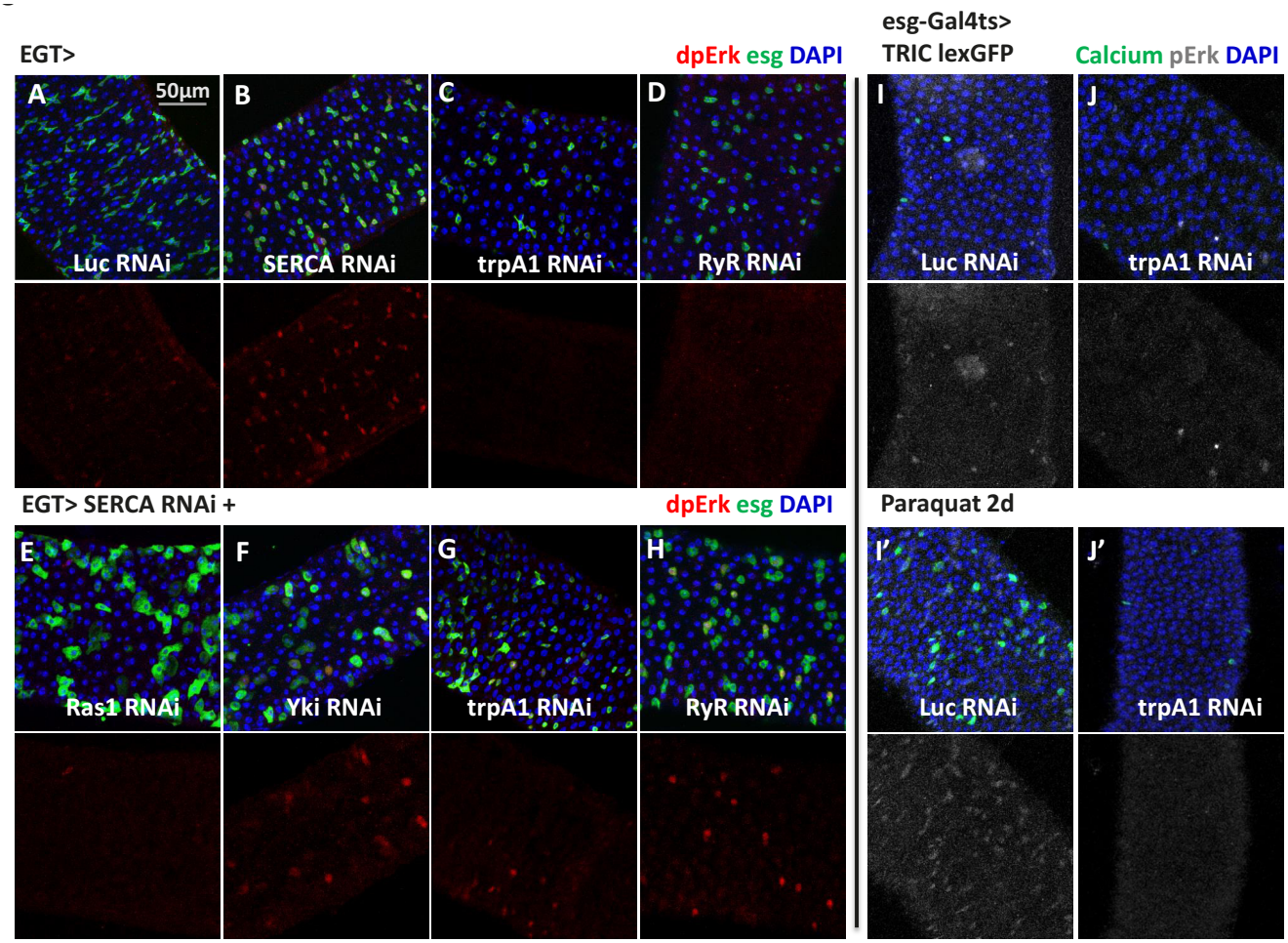


**Figure 6.** High cytosolic $Ca^{2+}$ is necessary and sufficient to activate Ras/MAPK in ISCs. (**A–D**) Midguts expressing *Luc* RNAi, *SERCA* RNAi, *trpA1* RNAi, or *RyR* RNAi in ISCs for 2-3d are stained for the Ras/MAPK activity marker dpErk. The channel of dpErk signal is shown below the merged image. Note *trpA1* RNAi group was imaged on a different date, but alongside *Luc* RNAi which exhibited the same level of pErk signal as the control group presented in A. (**E–H**) Midguts expressing *SERCA* RNAi together with *Ras1* RNAi, *Yki* RNAi, *trpA1* RNAi, or *RyR* RNAi in ISCs for 3d are stained for dpErk. The channel of dpErk signal is shown below the merged image. Note *trpA1* RNAi group in G was imaged on a different date together with C. (**I–J**) Midguts expressing the TRIC lexGFP reporter of intracellular calcium concentration and *Luc* RNAi or *trpA1* RNAi Luc in ISCs for 5d, with the last 2d feeding paraquat (**I'–J'**), are stained for dpErk. The channel of dpErk signal is shown to the right of the merged image. The TRIC lexGFP reporter consists of lexop-GFP, and two split modules of lexA whose assembly is dependent on intracellular calcium concentration.

DOI: 10.7554/eLife.22441.027

The following source data is available for figure 6:

**Source data 1.** Complete results for ***Figure 6—figure supplement 2H–I***.

DOI: 10.7554/eLife.22441.028

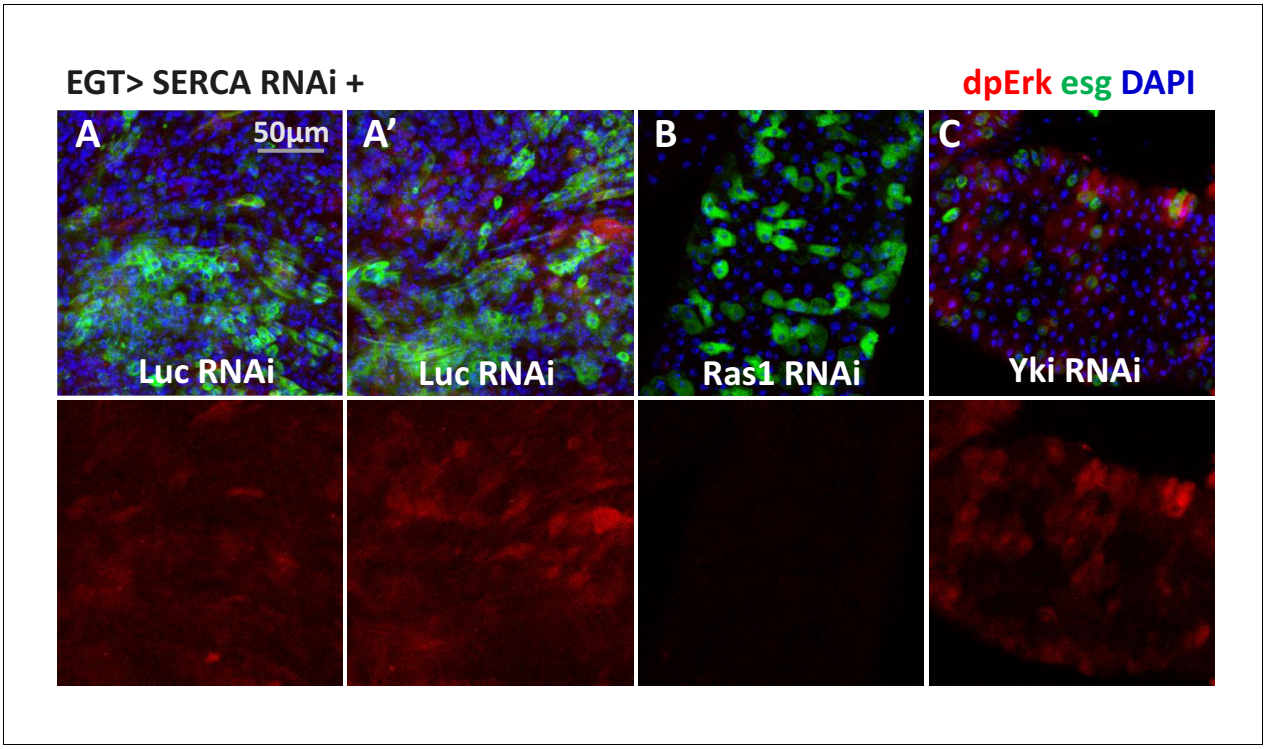


**Figure 6—figure supplement 1.** Prolonged induction of high cytosolic $Ca^{2+}$ in ISCs results in a nonspecific and variable pattern of Ras/MAPK activation. (**A–C**) Midguts expressing *SERCA* RNAi together with *Luc* RNAi, *Ras1* RNAi, or *Yki* RNAi in ISCs for 5d are stained for dpErk. The channel of dpErk signal is shown below the merged image. A and A' are biological replicates of the same genotype showing examples of variation. Although pErk induction is still detectable in some ISCs, the signal intensity varies among different ISCs and different midguts.

DOI: 10.7554/eLife.22441.029

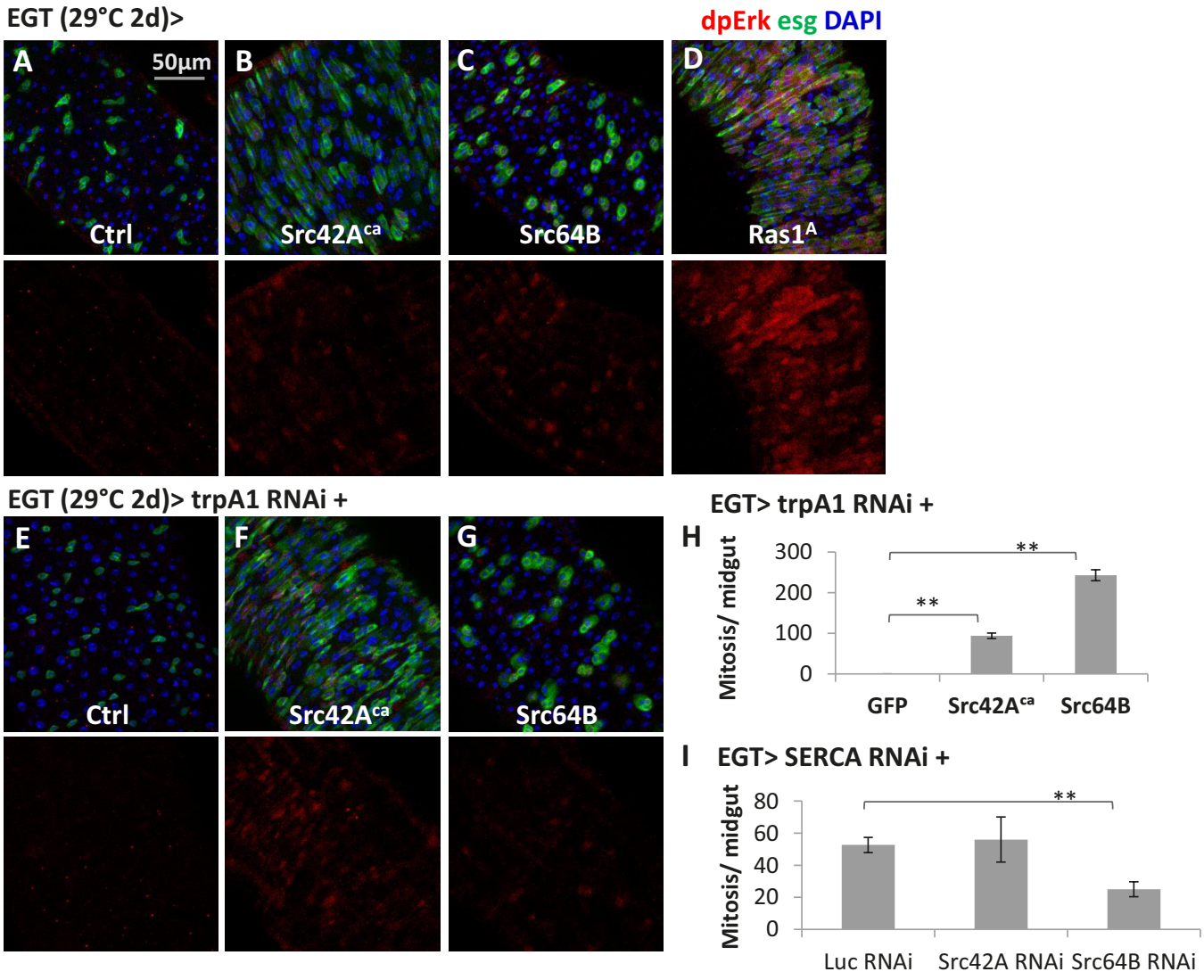


**Figure 6—figure supplement 2.** Src might be a mechanism by which cytosolic $Ca^{2+}$ can activate Ras/MAPK in ISCs. (**A–D**) Midguts expressing the constitutive active form of Src42A (Src42A$^{ca}$), Src64B, or Ras1$^{A}$ in ISCs for 2d are stained for the Ras/MAPK activity marker dpErk. The channel of dpErk signal is shown below the merged image. *w-* genetic background is used as the control for transgenic expression. (**E–G**) Midguts expressing *trpA1* RNAi alone or together with Src42A$^{ca}$/ Src64B in ISCs for 2d are stained for dpErk. The channel of dpErk signal is shown below the merged image. (**H**) Mitosis quantification of midguts expressing *trpA1* RNAi with GFP, Src42A$^{ca}$, or Src64B in ISCs for 3d. N > 5 midguts are analyzed for each genotype. Data are represented as mean ± SEM. (**I**) Mitosis quantification of midguts expressing *SERCA* RNAi with *Luc* RNAi, *Src42A* RNAi, or *Src64B* RNAi in ISCs for 4d. N > 4 midguts are analyzed for each genotype. Data are represented as mean ± SEM.

DOI: 10.7554/eLife.22441.030

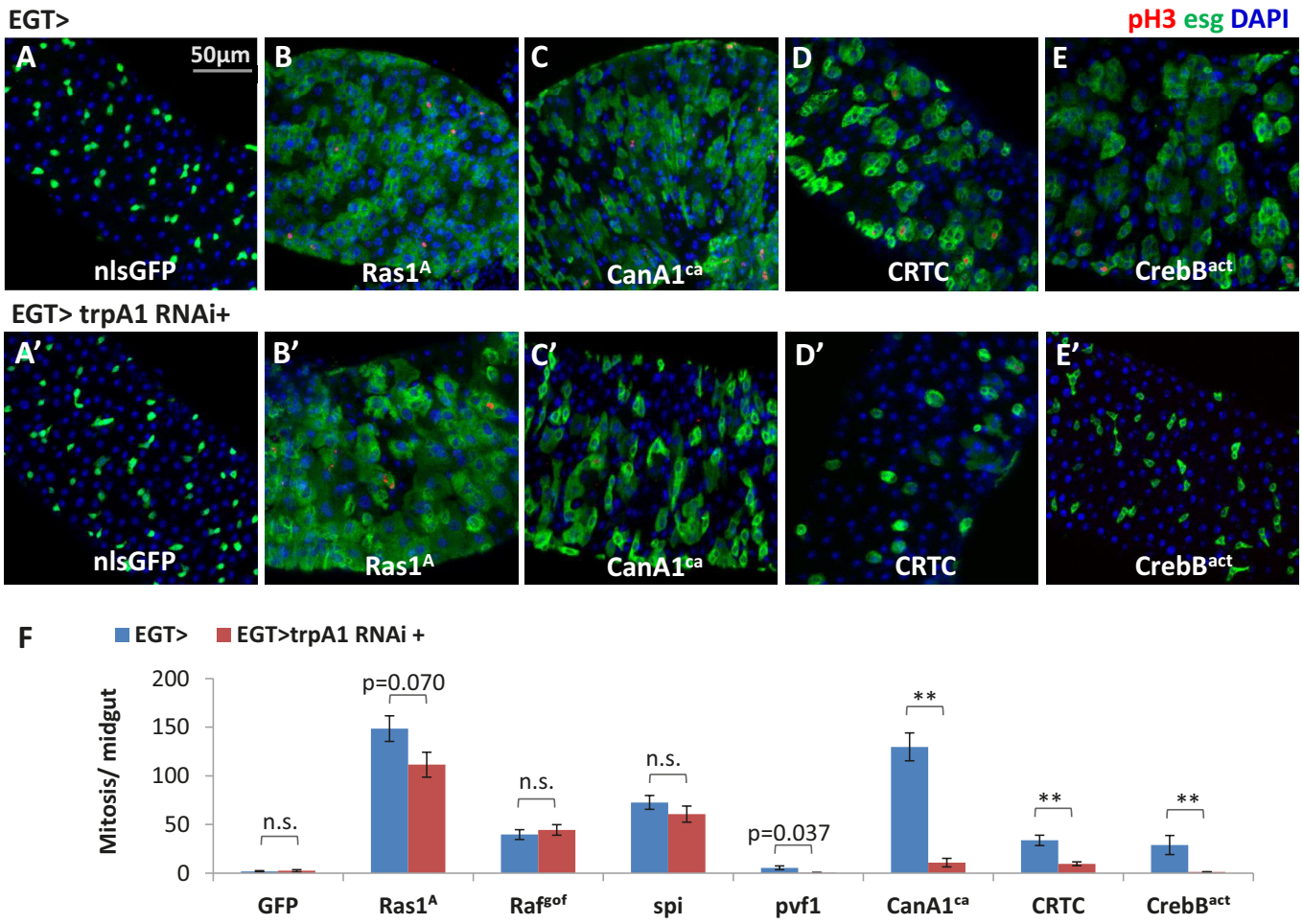


**Figure 7.** Ras/MAPK activity, not CanA/CRTC/CrebB, is sufficient for ISC proliferation in the absence of TRPA1. (**A–E**) Midguts over-expressing calcium responsive signaling molecules such as active Ras1 (Ras1A), constitutively active Calcineurin A1 (CanA1$^{ca}$), CREB-regulated transcription coactivator (CRTC), or active form of Creb (Creb$^{act}$) in ISCs for 5d are stained for the mitosis marker pH3. The expansion of esg>GFP signal by CanA1$^{ca}$ is reduced by *trpA1* RNAi, although not quite down to the wild-type level. This could be due to the different kinetics of two reagents, as CanA1$^{ca}$ may take effect sooner than *trpA1* RNAi. (**A'–E'**) Midguts expressing *trpA1* RNAi together with calcium-responsive signaling molecules in ISCs for 5d are stained for the mitosis marker pH3. (**F**) Mitosis quantification of midguts expressing GFP, Ras/ Raf, RTK ligands Spi/ Pvf1, CanA1$^{ca}$, CRTC, Creb$^{act}$, alone or together with *trpA1* RNAi for genetic epistasis analysis. N > 5 midguts are analyzed for each genotype. Data are represented as mean ± SEM. Although it has been reported that *pvf1* overexpression can increase ISC population (***Bond and Foley, 2012***), we could barely detect mitotic effect of Pvf1 in young adult flies.

DOI: 10.7554/eLife.22441.031

The following source data is available for figure 7:

**Source data 1.** Complete results for ***Figure 7F***, ***Figure 7—figure supplement 1F–G***.

DOI: 10.7554/eLife.22441.032

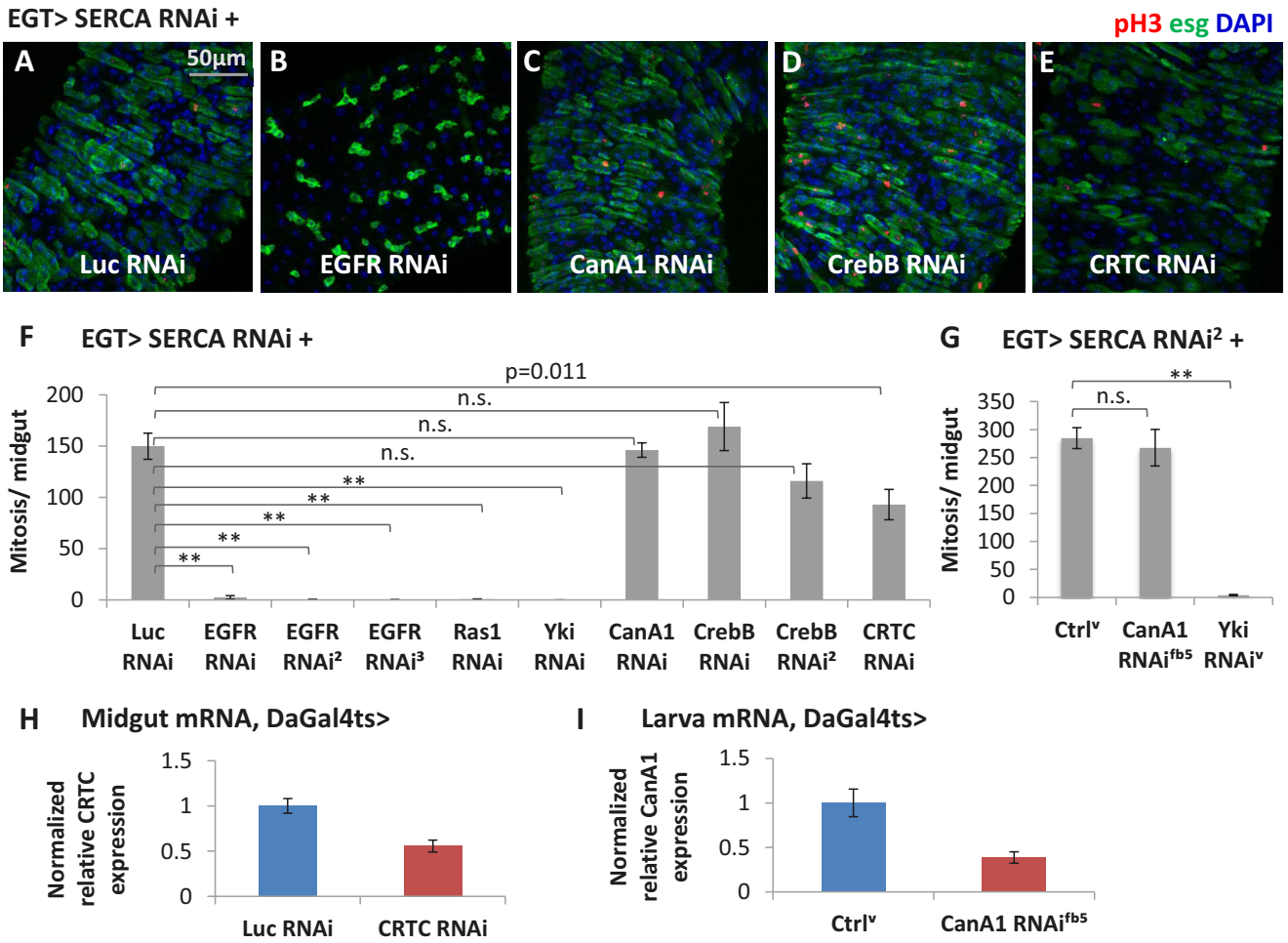


**Figure 7—figure supplement 1.** Ras/MAPK activity, but not CanA1/CrebB, is required for ISC proliferation induced by calcium influx. (**A–E**) Midguts expressing *SERCA* RNAi together with *Luc* RNAi, *EGFR* RNAi, *CanA1* RNAi, *CrebB* RNAi, or *CRTC* RNAi in ISCs for 3d are stained for mitosis marker pH3. (**F**) Mitosis quantification of midguts expressing *SERCA* RNAi together with *Luc* RNAi, *EGFR* RNAi (three different lines), *Ras1* RNAi, *Yki* RNAi, *CanA1* RNAi, *CrebB* RNAi (two different lines), or *CRTC* RNAi in ISCs for 5d. N > 7 midguts are analyzed for each genotype. Data are represented as mean ± SEM. (**G**) Mitosis quantification of midguts expressing *SERCA* RNAi$^2$ alone, or together with *CanA1* RNAi$^{fb5}$, or *Yki* RNAi$^v$ in ISCs for 5d. N > 5 midguts are analyzed for each genotype. Data are represented as mean ± SEM. For *CanA1* RNAi line 'fb5', flies with a similar w- genetic background carrying an empty insertional landing site (v60100) are used as the control (Ctrl$^v$). (**H**) RT-qPCR measurement of *CRTC* expression in midguts ubiquitously expressing *Luc* RNAi or *CRTC* RNAi for 5d. *GAPDH* and *rp49* are used for normalization. The data are presented as mean ± SEM for three technical replicates. (**I**) RT-qPCR measurement of *CanA1* RNAi $^{fb5}$ knockdown efficiency. L3 larvae expressing RNAi for 2 days are used for better quantification because midgut *CanA1* expression is barely detectable. *GAPDH* and *rp49* are used for normalization. The data are presented as mean ± SEM for three technical replicates.

DOI: 10.7554/eLife.22441.033

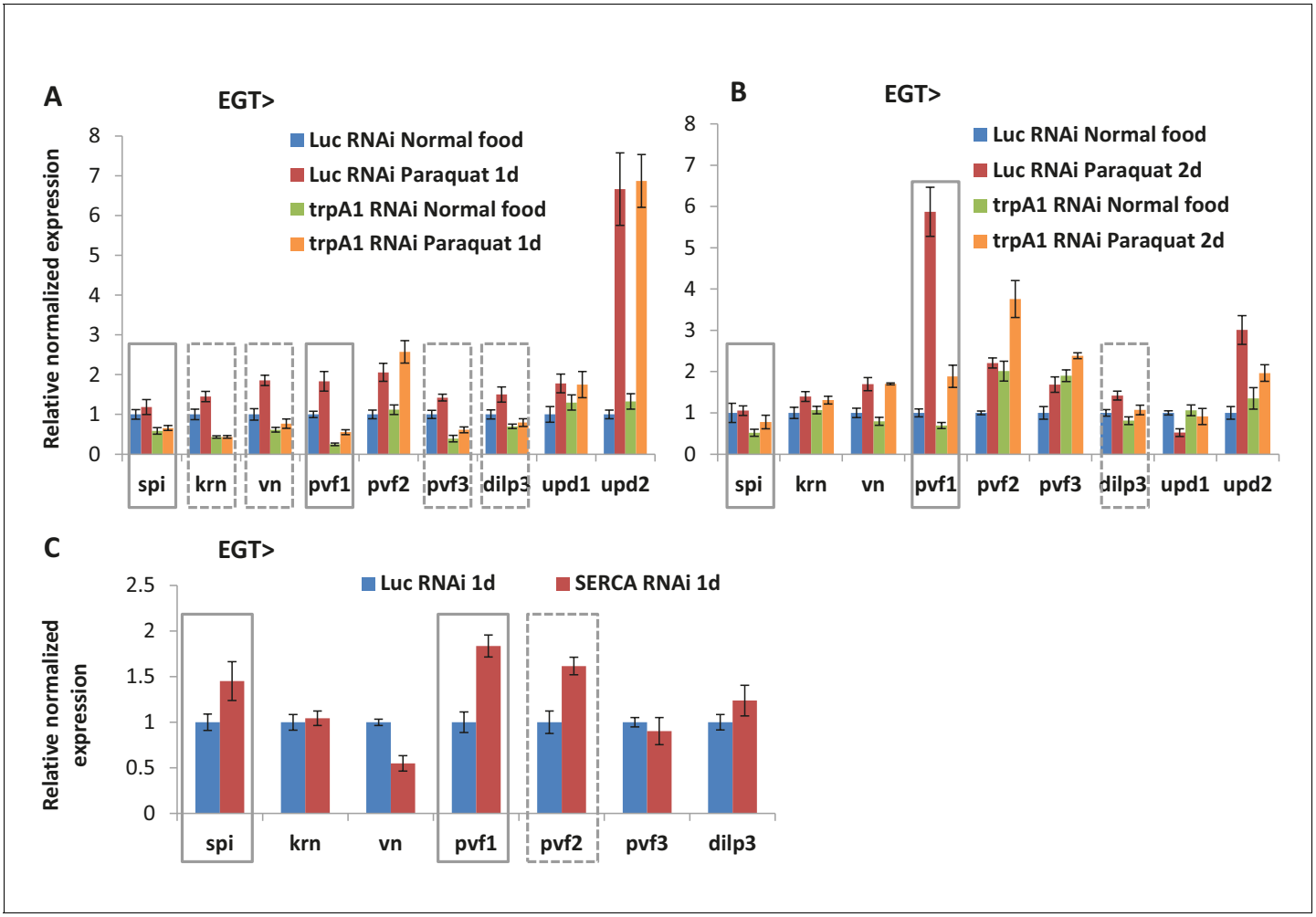


**Figure 7—figure supplement 2.** Ligands for receptor tyrosine kinases (RTKs) are affected by cytosolic $Ca^{2+}$ signaling. (**A**) RT-qPCR measurement of midguts expressing *Luc* RNAi or *trpA1* RNAi in ISCs for 6d, with the last day feeding on normal food or paraquat. *rp49* is used for normalization. The data are presented as mean ± SEM for three technical replicates. While expression of JAK/ Stat pathway ligands *upd1* and *upd2* remains unaffected, multiple RTK ligands (*spi*, *krn*, *vn*, *pvf1*, *pvf3*, *dilp3*, highlighted by gray square boxes) are down-regulated by *trpA1* RNAi. (**B**) RT-qPCR measurement of midguts expressing *Luc* RNAi or *trpA1* RNAi in ISCs for 9d, with the last 2d feeding on normal food or paraquat. *rp49* is used for normalization. The data are presented as mean ± SEM for three technical replicates. Note that only *spi*, *pvf1*, and *dilp3* are consistently down-regulated in *trpA1* RNAi groups in both (**A**) and (**B**). Different trends of *krn*, *vn*, and *pvf3* expression observed in (**B**) compared to (**A**) might suggest a delay, rather than reduction of these ligands by *trpA1* RNAi. (**C**) RT-qPCR measurement of midguts expressing *Luc* RNAi or *SERCA* RNAi in ISCs for 1d. Such early time point is chosen empirically to allow for efficient knockdown and avoid confounding effects of signaling pathway cross-activation at later stages of ISC proliferation. *rp49* is used for normalization. The data are presented as mean ± SEM for three technical replicates.

DOI: 10.7554/eLife.22441.034

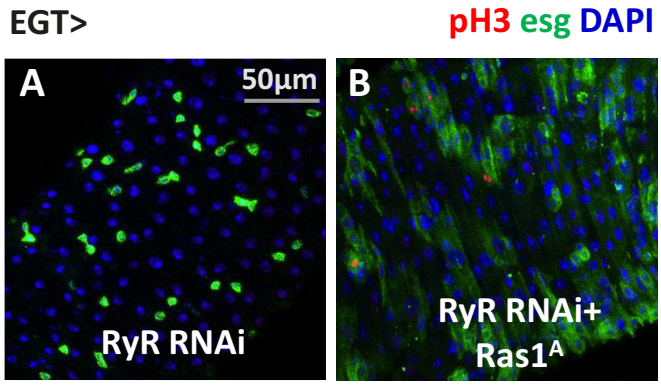


**Figure 7—figure supplement 3.** Ras/MAPK activity is sufficient for ISC proliferation in the absence of RyR. (**A–B**) Midguts, expressing *RyR* RNAi alone, or together with *SERCA* RNAi in ISCs for 5d, are stained for mitosis marker pH3.

DOI: 10.7554/eLife.22441.035

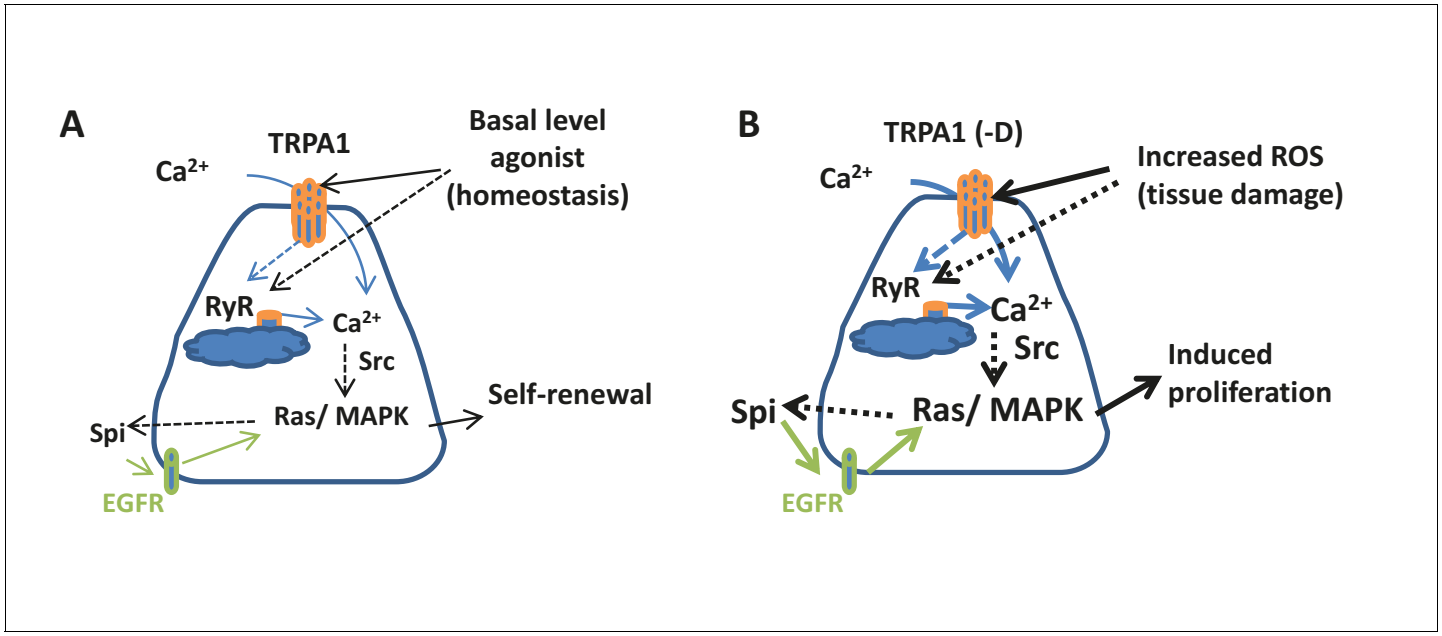


**Figure 8.** Connection between ROS, intracellular calcium, and stem cell activity. (**A**) Under tissue homeostasis conditions, basal levels of ROS and other unidentified stimuli can activate TRPA1 and RyR channels at low levels to allow low levels of cytosolic $Ca^{2+}$, autocrine EGFR ligand Spi, and Ras/MAPK activity required for stem cell self-renewal and minimal level of proliferation. Solid arrows indicate mechanisms that are either well-characterized (green) or demonstrated in this study; dashed arrows indicate unclear mechanisms inferred from literature or this study. (**B**) Under various tissue damage conditions, ROS levels dramatically increase and activate TRPA1, especially the D isoform. RyR channel can be activated either directly by ROS or by the initial $Ca^{2+}$ influx through TRPA1, allowing further calcium release from the ER to the cytosol. High levels of cytosolic $Ca^{2+}$ activate Ras/MAPK signaling via Src, and further amplify Ras/MAPK signaling via autocrine Spi-EGFR signaling. High EGFR-Ras/MAPK activity triggers ISC proliferation.
DOI: 10.7554/eLife.22441.036